Sensors and Actuators B 183 (2013) 388–394

Contents lists available at SciVerse ScienceDirect

Sensors and Actuators B: Chemical

journal homepage: www.elsevier.com/locate/snb

A multi-mode platform for cantilever arrays operated in liquid

Jason Jensen*, Niall Maloney, Martin Hegner*,[1]

Centre for Research on Adaptive Nanostructures and Nanodevices (CRANN) and School of Physics, Trinity College Dublin, Dublin 2, Ireland

ARTICLE INFO

Article history:
Received 25 October 2012
Accepted 28 March 2013
Available online xxx

Keywords:
Cantilever
Dynamic mode
Multifrequency
Static mode
Biosensor
Diagnostic

ABSTRACT

A rapid and reliable multi-mode device capable of the readout of both the static and dynamic response of a micron scale cantilever array in a physiological liquid environment is presented. The resolution of the static mode is on the order of 1–2 nm and in the dynamic mode it is possible to measure up to the 19th flexural resonance mode of vibration of a 500 μm long and 1 μm thick cantilever. Rapid measurement from the tip of the cantilevers or line scan measurement of the cantilever profiles are both possible in dual mode. The device provides sequential readout of both modes to provide the best signal to noise ratio for each mode. Proof of principle measurements are presented demonstrating the capabilities of the device and confirming the readout from both the static bending and multiple dynamic resonance modes.

1. Introduction

The improvement of silicon fabrication technologies over the last few decades and the introduction of the atomic force microscope (AFM) [1] created the availability of high quality, reproducible, and relatively inexpensive silicon cantilevers. Following from the AFM the interest in applying these micron scale cantilevers in other sensing applications has increased year on year. Biological applications for cantilever sensor arrays have been found in the fields of microbiology [2–6], genomics [7–9], proteomics [10–13] and many others.

The vast majority of applications using micron scale cantilevers utilise them in either the static or the dynamic mode. The static mode refers to the detection of the bending of the cantilever due to a stress induced preferentially on one surface of the cantilever when the target interacts specifically with a sensing layer. The dynamic mode refers to the detection of the change in the resonance frequency of the cantilever due to adsorption of mass, change in stiffness, or in the properties of the surrounding fluid.

Despite the large number of devices noted in the literature designed to use cantilever sensor arrays very few devices are capable of the readout of both the static and dynamic response of the cantilever array [14,15].

Many biological applications require working in a physiological fluid environment in order to probe the true mechanisms at work and to provide relevant and useful results. Thus, the aim of the development of any device to detect or investigate biological interactions using a mechanical sensor should be the continuous operation and readout of the device in a physiological liquid environment. The passing of the functionalised cantilever through a liquid to air interface should be avoided if the aim of the measurement is to investigate the interaction between biological molecules as the functionality or conformation of the molecules may be altered or damaged. In addition, passing the cantilever from a salt buffered solution to air will invariably lead to the formation of salt crystals on the surface of the cantilever which may lead to misinterpretation of the results obtained. Thus, the “dip and dry” method should be avoided. To allow bio-specific measurements and to deconvolute the real signal from the environmental influences a minimum of two sensors (a specific sensor and an in situ reference) have to be implemented. This requires multiple lasers or a movable laser source in the case where signals are optically read-out from the individual cantilever sensors [16].

There are many known challenges when operating a cantilever sensor in a liquid environment, especially in dynamic mode. In particular the large damping caused by the liquid causes low Q factors and thus lowers the sensitivity. The added mass of the liquid co-moved with the cantilever when it vibrates causes the effective mass of the cantilever to increase, and thus also lowers the sensitivity of the sensor. However, by operating the cantilever at its higher resonance modes some of the sensitivity can be regained [17–19].

The device presented here provides optical readout from both the static and dynamic modes of a cantilever array in a physiological liquid environment. The noise levels of the static mode are comparable to dedicated static mode devices and in the dynamic mode it is possible to read out up to the 19th flexural resonance mode. The device is user friendly, highly customisable, and requires little

* Corresponding authors. Tel.: +353 1 896 3141.
E-mail addresses: jensenja@tcd.ie (J. Jensen), hegnerm@tcd.ie (M. Hegner).
[1] Tel.: +353 1 896 2285.

0925-4005/$ – see front matter © 2013 Elsevier B.V. All rights reserved.
http://dx.doi.org/10.1016/j.snb.2013.03.133

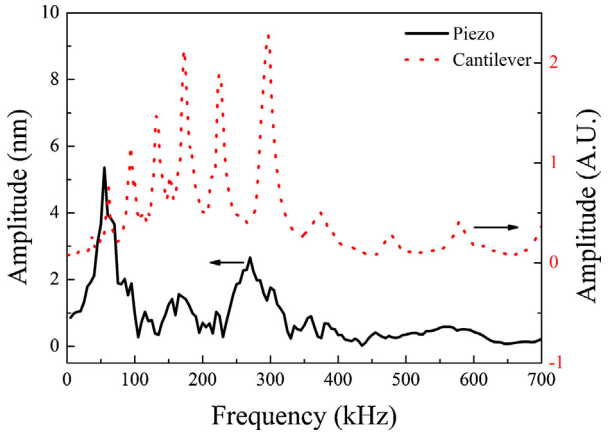

Fig. 1. Comparison between the amplitude of the piezo electric actuator and the actuated cantilever vs. frequency. It is clear from the overlay that the actuation of the cantilever does not create any non-flexural peaks in the response of the cantilever. The amplitude of the actuator vibration was measured using a laser doppler vibrometer (Polytec Fiber Vibrometer OFV-552, Polytec Ltd., Lambda House, Batford Mill, Harpenden Hertfordshire, AL5 5BZ, UK). The arrows in the graph indicate the relevant *y*-axis for each spectrum.

alignment of the laser on the array sensors once initially assembled.

2. Device details

The device presented is based on the principle of laser beam deflection to readout the static and dynamic response of an array of eight cantilevers. The main components of the device are the fluid chamber, the optics and laser positioning system, the position sensitive detector (PSD) and the fluidic system. The device is housed in a temperature stable environment and the device is controlled via PCI boards and a LabVIEW interface.

2.1. Fluid chamber

The chamber which houses the cantilever array is machined from PEEK (polyether ether ketone) and is designed such that the laminar flow of liquid is directed from the side and across the cantilevers in the array and minimises dead volume and areas of poor mixing. The total volume of the chamber is approximately 6 μl which is small enough to allow efficient changing of fluids (e.g. during sample injection) and minimise the amount of sample required. Low pressure fluid chromatography valves (Analytical Injection Loop D Uni, ECOM spol. s r.o., Americka 3, CZ12035 Praha 2, Czech Republic) allow efficient injection of analytes into the measurement chamber via sample loops.

The thermal motion of the cantilevers when immersed in liquid does not provide sufficient amplitudes of motion to allow measurement beyond the first few resonance modes of the cantilevers. In order to obtain the higher resonance modes the cantilevers are driven using a piezoelectric actuator (EBL Products Inc., East Hartford, CT 06108, USA). The cantilever array body is directly clamped on top of the piezoelectric actuator to allow coupling of the cantilevers and the actuator. The piezoelectric actuator does not create any non-flexural peaks in the frequency spectrum of the actuated cantilever (as shown in Fig. 1).

The piezoelectric actuator is separated from the liquid chamber by a thin membrane which provides a barrier between the liquid and the piezoelectric actuator to avoid shorting and damage.

The cantilever array is positioned at an angle of 45° to the edges of the chamber to avoid the creation of additional noise in the frequency spectra due to the formation of standing waves in the liquid or reflections from the walls of the chamber

A heat pulse can be applied to the fluid chamber by passing a current through two 15 Ω resistors connected in series and located below the fluid chamber. This allows calibration of the response of the individual cantilevers in the array and results in comparable measurements between the cantilevers.

2.2. Optics and laser positioning system

A single wavelength fibre coupled laser (632.99 nm, free space power >2.4 mW, SWL 7504-P; Newport, CA 92606, USA) is collimated into a 3.5 mm beam diameter (F280 APC-B; Thorlabs, Cambridgeshire, CB7 4EX, UK). The output of the laser was attenuated using a neutral density filter (OD 1.3 NE513B; Thorlabs) to avoid saturating the PSD. The beam is focused into a 12 μm diameter spot on the surface of the cantilever using a 50 mm focal length achromatic doublet (AC254-050-A1-ML; Thorlabs). The depth of focus of the beam is ~340 μm. The optic axis of the system is maintained using a cage system [30 mm Cage mount: CP02B; Collimator Mounting adapter: AD11F; Cage Plate: CP02/M; Rods: ER2; Filter Holder: NE513B] (Thorlabs). The laser has a very stable output and is temperature controlled which avoids any changes in power that can be observed when using an array of VCSELs for readout.

Two automated translation stages (M110.1DG & M122.2DD; Physik Instrumente, Bedford, MK43 0AN, UK) allow the sequential readout of the response from the eight cantilevers in the array. The stages are aligned at right angles to each other to provide movement between the cantilevers and also along the length of each cantilever. The positioning stages facilitate rapid movement between cantilevers (max travel speeds 1 and 20 mm/s respectively), with a unidirectional repeatability of 100 and 150 nm respectively and a minimal step size of 50 and 200 nm respectively to provide very repeatable positioning of the spot on the surface. This allows low noise levels in static mode (~1–2 nm) and also does not affect the dynamic mode.

The second positioning stage combined with the small spot size of the laser allows the best position for readout of each dynamic mode to be found on each cantilever in the array. Individual positioning along each cantilever compensates for small differences between the cantilevers and as a result more cantilevers in the array can be readout successfully during each experiment. Previously, using a VCSEL (Vertical Cavity Surface Emitting Laser) array or a single translation stage, it was not always possible to have low noise/high amplitude readings from all cantilevers in the array because the higher resonance nodes are not necessarily at exactly the same distance from the tip of each cantilever. The second automated stage also provides easy use of arrays containing different numbers of cantilevers, different length cantilevers (harp shaped arrays), or cantilevers with different properties (e.g. thickness, width).

The two automated stages are connected to a lockable xyz micro-translation stage (Gothic Arch 9061-XYZ; Newport, CA 92606, USA) which allows fine focusing of the laser spot on the surface of the cantilever.

The stable optical system allows for ease of use of the device. Once the laser has been aligned the array and the fluid chamber can be removed and replaced many times without any need for adjustment of the optics. The focus of the laser has not needed adjustment since the initial alignment (>1 year).

The various stages and optical cage system are connected using custom machined pieces and the entire system is mounted on a breadboard (MB1530M, Thorlabs)

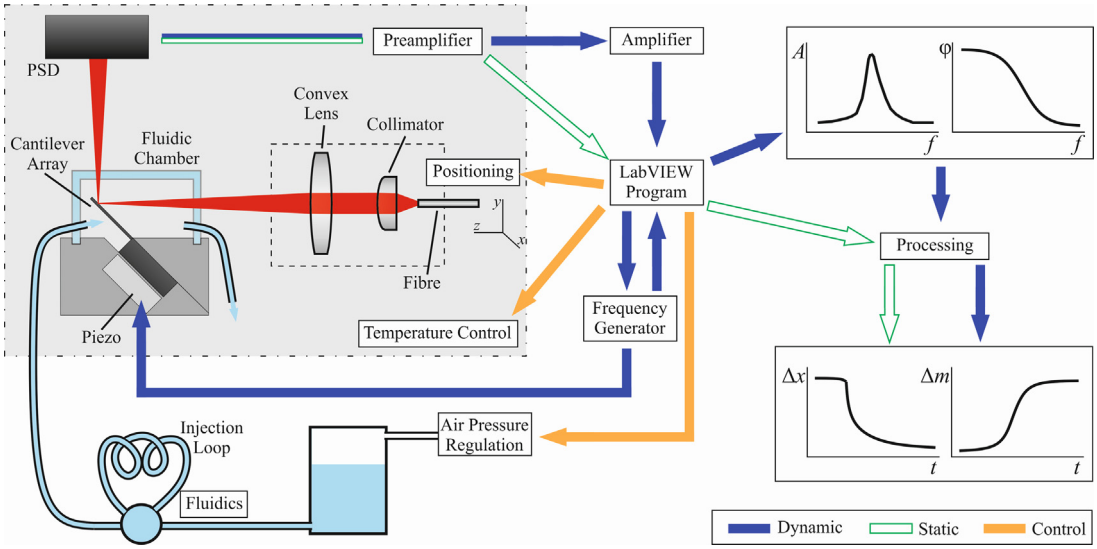

Fig. 2. Schematic of experimental device and measurement procedure. The main LabVIEW program controls all aspects of the device and the acquisition of data. Using the device it is possible to record both the dynamic and the static response of the individual cantilevers in the array. The LabVIEW program controls the heating and cooling of the box containing the device to maintain a stable temperature to within ±0.1 °C. The flow of liquid through the fluid chamber via air pressure is also controlled using the LabVIEW program. Following the dynamic measurement (blue arrows) amplitude (A) and phase (φ) frequency spectra are output by the LabVIEW program. Following this the static signal (green arrows on the schematic) is recorded and the LabVIEW program then determines the bending of the cantilever. The resonance modes and bending of each cantilever are obtained sequentially before moving to the next cantilever in the array. The dynamic and static data can then be processed using NoseTools or a similar routine to obtain the change in mass (Δm) and the change in bending (Δx) or surface stress of the cantilever with respect to time (t). (For interpretation of the references to color in this figure legend, the reader is referred to the web version of this article.)

2.3. Temperature control and fluidic system

A steady temperature is essential when working with cantilevers which are coated on one side with a metal. Any change in temperature in the system will induce a bending in the cantilevers due to the difference in thermal expansion coefficients of the metal and the silicon. To avoid this the entire device is housed inside a small refrigeration unit (Intertronic, Interdiscount, Switzerland) which is maintained at a constant temperature of 23.0 ± 0.1 °C via a fuzzy logic routine implemented in the main LabVIEW program.

A custom air pressure driven fluid flow system is controlled via LabVIEW. The system comprises of custom made glass bottles with an air inlet at the top of the bottle and a fluid outlet at the bottom of the bottle. The fluid is caused to flow through the chamber by applying pressure to the bottle. The pressure is monitored using a pressure sensor (140 PCB, Sensor Technics, McGowan House, 66C Somers Road, Rugby, Warwickshire CV22 7DH, United Kingdom). The flow of air to and from the bottles is controlled by switching valves (EV2 & EV3, Clippard, Parc Scientifique Einstein, Rue du Bosquet, 6, B-1348 Louvain-la-Neuve-Sud, Belgium) controlled via the main LabVIEW program and a mechanical relay board (NI PCI-6520, National Instruments, Texas, USA). The pressure applied to the bottles can be either positive (pushed flow) or negative (pulled flow) depending on the setting of the valves and the connection to the compressed air regulator (0–50 mbar,U33, Spectrotec, Spectron Gas Control Systems GmbH, Fritz-Klatte-Str. 8, D-65933 Frankfurt) or a vacuum pump. In the current device it is possible to control the flow for up to four bottles.

2.4. Actuation and Readout

As shown in the schematic in Fig. 2 the response of the cantilevers is obtained using optical beam deflection readout. The position of the reflected beam was measured using a 10 mm linear PSD (IL10-10-ASU15, Sitek, Partille, Sweden). The resonance modes and bending of each cantilever are obtained sequentially. The wait time before obtaining the bending is significantly longer than the damping time of the vibration of the cantilever and therefore there is no additional noise in the static signal due to the dynamic readout.

2.4.1. Dynamic signal

The laser spot is moved to one of the nodes of the vibration, which can vary in position depending on local material properties, along the length of the cantilever using the second automated stage controlled by a LabVIEW (National Instruments) program. The cantilevers are excited at their flexural resonance modes by providing a linear frequency sweep from a frequency generation board mounted in a PC (NI PCI 5406, National Instruments) controlled by the LabVIEW program. The output from the PSD is converted to a voltage signal and preamplified using standard custom electronics mounted on the back of the PSD housing unit. The voltage signal is then amplified (SR560 Low-Noise Preamplifier; Stanford Research Systems, CA 94089, USA) and digitised (NI PCI 5112; National Instruments) before being analysed in the LabVIEW program against the output from the frequency generator to create amplitude and phase frequency spectra. The readout of the dynamic signal has been optimised using a circular data buffer to allow measurement of >3000 data points in each spectrum for eight cantilevers in ∼ 30 s (including travel between cantilevers). The sampling rate is set to 10^7 samples s^{-1} to satisfy Nyquist's theorem and avoid aliasing. Each data point in the spectrum is the average of 10^4 samples.

2.4.2. Static signal

The laser spot is moved to the tip of the cantilever using the second automated translation stage. The differential and sum signals are then obtained after a small wait (150 ms) to avoid any vibrations due to movement and to ensure the cantilever is no longer vibrating from the dynamic measurement. The signal from the PSD is then passed to the LabVIEW program via a data acquisition board (DAQ, NI PCI 6221, National Instruments). The mean differential and sum (2500 samples at a rate of 10^5 samples s^{-1}) are then used to

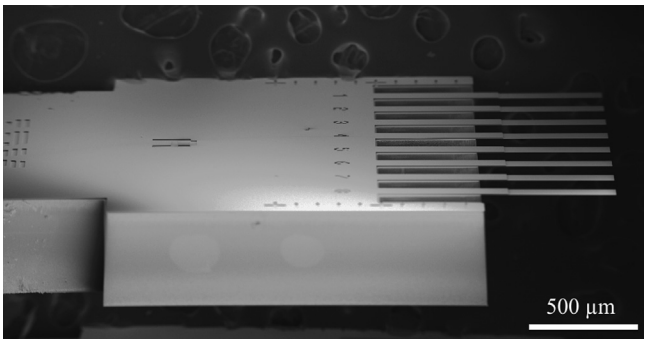

Fig. 3. A typical cantilever array used in the experiments. The cantilevers have a length of 500 μm, a width of 100 μm and a thickness of 1 μm. The hinged portion of the cantilever is 120 μm long and ~3 μm thick. The centre to centre spacing of the cantilevers is 250 μm.

calculated the bending (x) of the cantilever using the following formula

$$x = \frac{I_1 - I_2}{I_1 + I_2}\frac{L}{2}G \quad (1)$$

where $(I_1 - I_2)$ and $(I_1 + I_2)$ are the differential and sum signals from the PSD, L is the length of the PSD and G is the calibration factor. The G factor calculated for the device is 3125 using a geometric method. For finer calibration and for use with more sensitive measurements the G factor can be found using a thermal method as outlined in [20].

It is also possible to obtain a line profile of the bending of the cantilever by taking measurements at regular intervals along the length of the cantilever. The profile can be obtained from the PSD signals using the following formula [21]

$$x(\delta) = \frac{1}{2D}\int_0^{\delta} s(\delta')d\delta' - \frac{1}{4}\frac{\delta^2}{D}\cos\ \alpha \quad (2)$$

where $x(\delta)$ is the profile along the longitudinal axis, D is the distance between the cantilever and the PSD, α is the angle between the laser and the cantilever normal, and $s(\delta)$ is the displacement of the laser spot on the PSD.

When only the static signal is being recorded it is possible to read out from all eight cantilevers once every 6–7 s.

3. Experimental

3.1. Cantilever arrays

The cantilever arrays used in the measurements presented were Si cantilever arrays (orientation: 110) with eight cantilevers per array (IBM Research Laboratory, Rüschlikon, Switzerland). The cantilevers have a length of 500 μm, width of 100 μm and a thickness of 1 μm. The centre to centre spacing of the cantilevers is 250 μm. A scanning electron microscope (SEM, Zeiss Ultra, Cambridge, UK) image of a typical cantilever array used in the experiments is shown in Fig. 3.

3.2. Metal coating

A gold layer on the top surface of the cantilever facilitates easy functionalisation using thiol chemistry, increases the reflectivity of the surface to aid in optical deflection, and also can be used to calibrate the sensors for deflection measurements when a heat pulse is applied to the fluid chamber.

The surface of the cantilevers was coated with a 4 nm Ti adhesion layer and 9 nm of Au for the heat pulse experiments. For the oligo and bead experiments a 2 nm Ti adhesion layer and a 21 nm functional Au layer were used.

The metals were deposited using electron beam evaporation (Temescal FC-2000 Evaporation System, Scotech, Netherton Road, Lanqank, Renfrewshire, Scotland PA14 6YG). The Ti was deposited at a rate of 0.2 Å/s and the Au was deposited at a rate of 0.5 Å/s.

Prior to metal deposition the cantilever arrays were cleaned using a short 5 min light O_2 plasma etch (settings: 0.3 mbar O_2, 160 W, 40 kHz) followed by soaking for 5 min in HPLC grade ethanol (Sigma–Aldrich, Arklow, Ireland).

3.3. Biotinylated oligo binding streptavidin coated polystyrene beads

The aim of this experiment was to demonstrate the sensitivity of the device to both stress and mass change on the surface. This was achieved by measuring the bending induced by hybridisation of a biotinylated target oligo and the mass uptake due to the subsequent binding of streptavidin coated polystyrene beads.

3.3.1. Functionalisation

The Au coated array was pre-cleaned using UV radiation (5 min, UV Clean 135500, Boekel, 855 Pennsylvania Blvd, Feasterville, PA. 1905, USA) followed by soaking in HPLC grade ethanol for 5 min [22]. The cantilevers were either functionalised with the probe oligo (thiol – $(CH_2)_6$ – 5′-ATC ACA CTG TAG CGA-3′, Microsynth AG, Schützenstrasse 15, P.O. Box 9436, Balgach, Switzerland) or the unspecific reference oligo (thiol – $(CH_2)_6$ – 5′-ACA CAC ACA CAC-3′) at a concentration of 10 μM in 50 mM Triethylammonium acetate (TEAA, Sigma-Aldrich, Arklow Ireland). The cantilevers were functionalised for 30 min using the capillary immersion method followed by a rinse in a 50 mM TEAA solution for 5 min and a rinse in 1× Gibco PBS (Invitrogen, via Biosciences, Bio-Sciences, 3 Charlemont Terrace, Crofton Road, Dun Laoghaire, Co. Dublin, Ireland) for 5 min.

3.3.2. Measurement

The array was loaded into the fluid chamber and allowed to equilibrate in the buffer (1× Gibco PBS, flow rate 40 μl/min). Once the temperature was stable the flow was stopped and the cantilevers were allowed to equilibrate again. A heat pulse was applied to the fluid chamber (2 V, 2 min) for calibration of the sensors. The array was allowed to equilibrate once more before injection of the target oligo.

The biotinylated target oligo (Bio – $(CH_2)_6$ – 5′-TCG CTA CAG TGT GAT-3′) was injected into the chamber at a concentration of 20 nM in 1× Gibco PBS at a flow rate of 40 μl/min for 90 s. The flow was then turned off for 30 min before rinsing the chamber for 10 min at a rate of 80 μl/min.

A baseline for the frequency was then recorded before injecting streptavidin coated polystyrene beads at 40 μl/min for 90 s (1.87 μm diameter, 5×10^3 beads/μl in 1× Gibco PBS, Spherotech, Inc., 27845 Irma Lee Circle, Unit 101, Lake Forest, IL 60045, USA). After 45 min the chamber was rinsed at 80 μl/min for 20 min.

4. Results and discussion

4.1. Resonance spectra

The resonance spectrum from one of the cantilevers in a typical array is shown in Fig. 4. The flexural resonance modes from 2 to 19, between 1 and 1400 kHz, are indicated in the amplitude spectrum. The first mode is not observed in the spectrum due to its low frequency and amplitude in liquid (~900 Hz) which was observable in the frequency window measured. The spectrum was obtained in one measurement lasting 3 s and has not been filtered or smoothed. Using previous generations of dynamic mode devices it would be

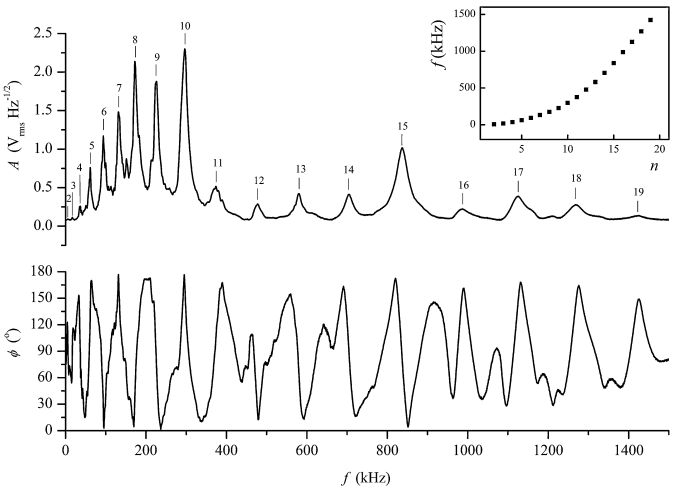

Fig. 4. Amplitude and phase resonance spectra of a typical cantilever from the arrays used in the device. The flexural resonance modes from 2 to 19 are clearly visible in the frequency range 1–1400 kHz. Inset: The approximately squared dependence of the frequency f on the mode number n of the resonance peaks confirms that the modes observed are the flexural resonance modes.

necessary to take several measurements and combine them afterwards to achieve such a spectrum. This demonstrates the speed, sensitivity and ease of use of the device in the dynamic mode of operation.

4.2. Line profile of a cantilever

To demonstrate the sensitivity of the dynamic mode to the positioning of the laser spot on the surface of the cantilever a scan along the longitudinal axis of a typical bare silicon cantilever was performed with measurements taken every 5 μm. For the dynamic measurements the cantilever was excited at its 5th flexural resonance mode in air and the resonance spectra were fitted with a simple harmonic oscillator model to determine the amplitude of the signal. The static bending profile was obtained from the PSD signal using Eq. (2). The profiles are shown in Fig. 5. The nodes and antinodes of the resonance [23] are clearly reflected in the dynamic profile, with the maximum signal obtained at the nodes of resonance. The bending profile shows a 3 μm upwards bend of the cantilever indicating a small residual tensile stress from the

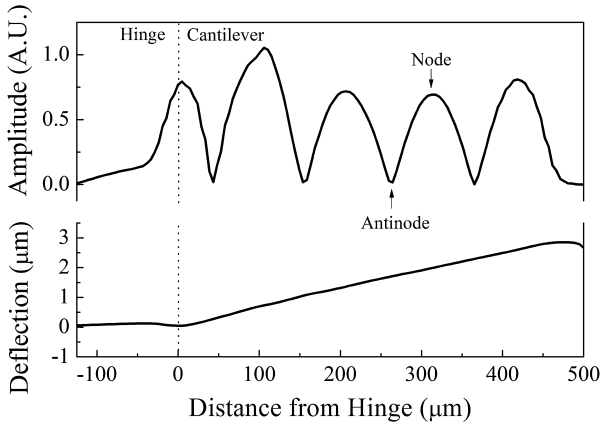

Fig. 5. Measurement of the amplitude of the 5th resonance mode in air and the bending of a typical cantilever from the array. The data was obtained by taking a dynamic measurement followed by a static measurement at 5 μm intervals along the length of the cantilever and the bending profile can be established using Eq. (2). The 120 μm long and ~3 μm thick hinged portion of the cantilever has some flexibility as indicated by the reduced amplitude of vibration observed [26].

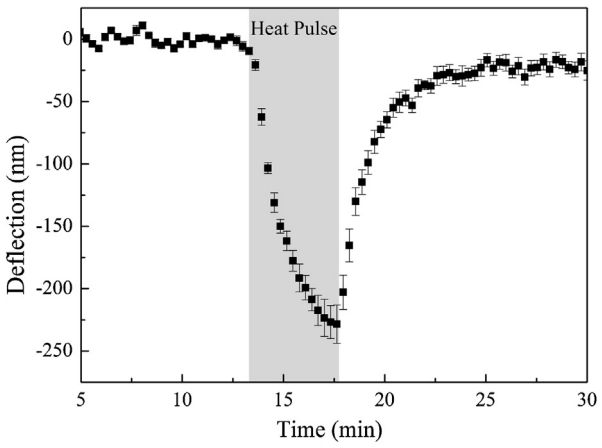

Fig. 6. Average static response of the eight cantilevers in the array to the 250 s heat pulse. The cantilevers showed an average bending of 230 nm by the end of the heat pulse.

fabrication process. The bending profile was calibrated using the thick side bar as a reference to account for any tilt of the cantilever in the holder.

4.3. Heat pulse

To demonstrate the sensitivity of the device to both dynamic and static response of the cantilever array a heat pulse was applied to the fluid chamber (2 V, 250 s). This caused a trough to be formed in the static signal (as shown in Fig. 6) which can be used to calibrate the mechanical response of the individual cantilevers in the array and allow for comparable measurements between the cantilevers [24]. The downward bending is caused by the different thermal expansion coefficients of the silicon cantilever and the gold layer on the upper surface of the cantilever ($3 \times 10^{-6}\,^{\circ}C^{-1}$ for Si and $14 \times 10^{-6}\,^{\circ}C^{-1}$ for Au).

The flexural resonance modes 8–10 were recorded during the heat pulse and their response is shown in Fig. 7. The shift in resonance frequency is due to the change in properties of the surrounding fluid with increase in temperature and the stress generated near the hinge. The higher modes of resonance are more sensitive as expected [17].

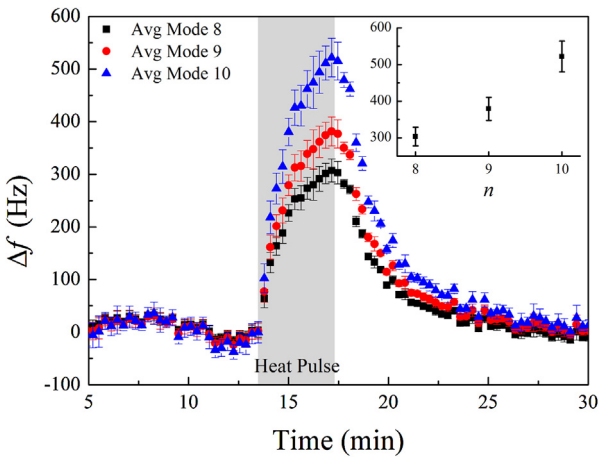

Fig. 7. Average frequency response of the flexural resonance modes 8–10 to the 250 s heat pulse. Inset: the maximum frequency shift vs. mode number. It is clear that the higher resonance modes are more sensitive to an applied stimulus.

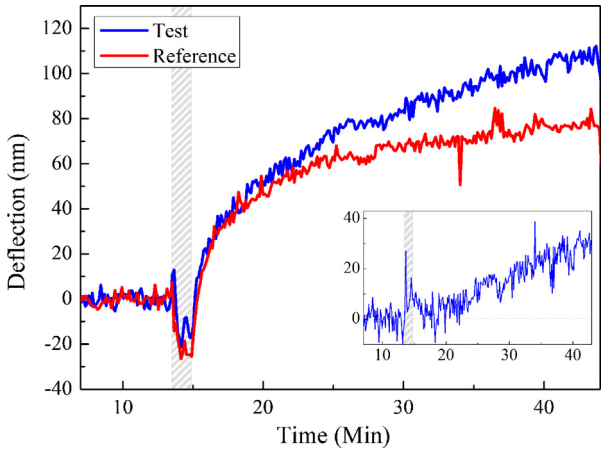

Fig. 8. Static mode averaged response to injection of 20 nM biotinylated target oligo. The injection point is indicated by the hatched area of the graph. There is a clear difference in the response of the blue (upper) test cantilevers to the red (lower) reference cantilevers. The inset graph shows the differential response (reference subtracted) of the test cantilevers. There was an average differential bending of 30 nm following the hybridisation of the biotinylated target oligo to the probe oligo on the top surface of the test cantilevers after 30 min. (For interpretation of the references to color in this figure legend, the reader is referred to the web version of this article.)

4.4. Biotinylated oligo binding streptavidin coated polystyrene beads

The static signal from the cantilevers in the array was normalised according to the calibration heat pulse test as outlined in [25]. The averaged response of the test and reference cantilevers to injection of the 20 nM target biotinylated oligo is shown in Fig. 8. The two sets of cantilevers show a clear difference in response to the hybridisation of the target oligo. The differential response indicates that there is a difference of 30 nm in the average bending of the two sets of cantilevers which is within the range expected for this type of cantilever array.

Following the injection of the target oligo the streptavidin coated beads were injected into the fluid chamber. Fig. 9 indicates that there was an overall average mass increase on the surface of the test cantilevers of 900 ± 100 pg when the reference signal has been subtracted. The noise levels of the mass response of the cantilevers were larger when the beads were present in the fluid chamber. This is due to the beads interfering with the path of the beam when they pass through it. The noise levels reduce to a similar level as before following the rinse of the chamber.

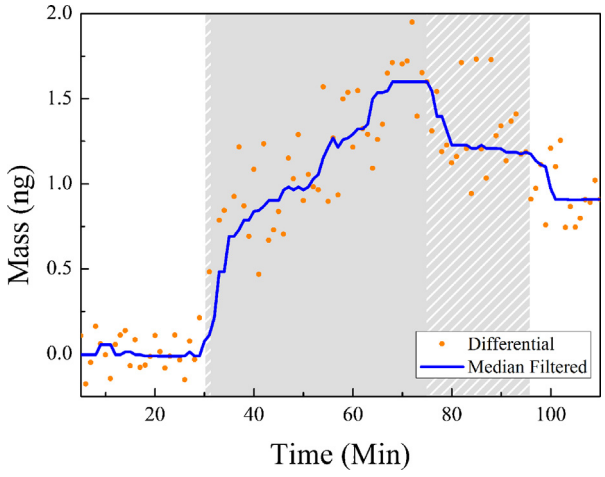

Fig. 9. Averaged differential (reference subtracted) response of the test cantilevers following injection of the 5×10^3 beads/μl streptavidin coated polystyrene beads. The hatched areas indicate the injection of the beads (40 μl/min) and the rinsing of the chamber (80 μl/min). The shaded area of the graph indicated the time when the beads are present in the fluid chamber. The noise levels of the frequency response are higher when the beads are in the chamber due to scattering of the beam by the beads. There is a clear increase of mass on the surface of the test cantilevers corresponding to 900 ± 100 pg. The quantitative noise level of the base line is ±150 pg.

5. Conclusion

The device presented is capable of rapid and reliable readout of both the static and dynamic response of a cantilever array in a physiological liquid environment. The static mode resolution of the device is on the order of ~2 nm when using a 1 μm thick cantilever. Using the dynamic mode it is possible to readout up to the 19th flexural resonance mode of a 500 μm long and 1 μm thick cantilever. The static and dynamic response of eight cantilevers can be obtained in 30 s with good signal to noise levels from the tip of the cantilevers and line scan analysis of the cantilevers is also possible. A proof of concept experiment was presented indicating the robustness of the device and the potential applications that can be used. While the limits of detection and absolute bending measured are dependent on the particular cantilevers chosen for a particular experiment, the device presented here is easily customisable and can provide readout from virtually any 2D array of micron scale cantilevers while providing a temperature stable environment with control over fluid flow through the chamber integrated into the user friendly LabVIEW program.

Acknowledgements

The SEM images were taken in the Advanced Microscopy Laboratory, Trinity Technology and Enterprise Campus, Dublin 2, Ireland under the framework of the INSPIRE programme, funded by the Irish Government's Program for Research in Third Level Institutions, Cycle 4, National Development Plan 2007–2013. This work was supported by Science Foundation Ireland under the CSET scheme SFI08/CE/I1432 and PI scheme SFI/09IN/1B2623.

References

[1] G. Binnig, C.F. Quate, C. Gerber, Atomic force microscope, Physical Review Letters 56 (1986) 930.
[2] B. Ilic, Y. Yang, H.G. Craighead, Virus detection using nanoelectromechanical devices, Applied Physics Letters 85 (2004) 2604–2606.
[3] N. Nugaeva, K.Y. Gfeller, N. Backmann, H.P. Lang, M. Duggelin, M. Hegner, Micromechanical cantilever array sensors for selective fungal immobilization and fast growth detection, Biosensors and Bioelectronics 21 (2005) 849–856.
[4] K.Y. Gfeller, N. Nugaeva, M. Hegner, Micromechanical oscillators as rapid biosensor for the detection of active growth of *Escherichia coli*, Biosensors and Bioelectronics 21 (2005) 528–533.
[5] D. Ramos, J. Tamayo, J. Mertens, M. Calleja, L.G. Villanueva, A. Zaballos, Detection of bacteria based on the thermomechanical noise of a nanomechanical resonator: origin of the response and detection limits, Nanotechnology 19 (2008) 035503.
[6] N. Maloney, G. Lukacs, N. Nugaeva, W. Grange, J.P. Ramseyer, J. Jensen, M. Hegner, Fibre optic readout of microcantilever arrays for fast microorganism growth detection, Journal of Sensors 2012 (2012) 405281.
[7] R. McKendry, J.Y. Zhang, Y. Arntz, T. Strunz, M. Hegner, H.P. Lang, M.K. Baller, U. Certa, E. Meyer, H.J. Guntherodt, C. Gerber, Multiple label-free biodetection and quantitative DNA-binding assays on a nanomechanical cantilever array, Proceedings of the National Academy of Sciences of the United States of America 99 (2002) 9783–9788.
[8] J. Fritz, M.K. Baller, H.P. Lang, H. Rothuizen, P. Vettiger, E. Meyer, H.-J. Güntherodt, C. Gerber, J.K. Gimzewski, Translating biomolecular recognition into nanomechanics, Science 288 (2000) 316–318.
[9] J. Mertens, C. Rogero, M. Calleja, D. Ramos, J.A. Martin-Gago, C. Briones, J. Tamayo, Label-free detection of DNA hybridization based on hydration-induced tension in nucleic acid films, Nature Nanotechnology 3 (2008) 301–307.
[10] P.S. Waggoner, M. Varshney, H.G. Craighead, Detection of prostate specific antigen with nanomechanical resonators, Lab on a Chip 9 (2009) 3095–3099.

[11] N. Backmann, C. Zahnd, F. Huber, A. Bietsch, A. Pluckthun, H.P. Lang, H.J. Guntherodt, M. Hegner, C. Gerber, A label-free immunosensor array using single-chain antibody fragments, Proceedings of the National Academy of Sciences of the United States of America 102 (2005) 14587–14592.
[12] T. Braun, M.K. Ghatkesar, N. Backmann, W. Grange, P. Boulanger, L. Letellier, H.P. Lang, A. Bietsch, C. Gerber, M. Hegner, Quantitative time-resolved measurement of membrane protein-ligand interactions using microcantilever array sensors, Nature Nanotechnology 4 (2009) 179–185.
[13] J. Jensen, M. Farina, G. Zuccheri, W. Grange, M. Hegner, Quantitative, label-free detection of the aggregation of alpha-synuclein using microcantilever arrays operated in a liquid environment, Journal of Sensors 2012 (2012), http://dx.doi.org/10.1155/2012/874086, Article ID 874086, 7 pages.
[14] F.M. Battiston, J.P. Ramseyer, H.P. Lang, M.K. Baller, C. Gerber, J.K. Gimzewski, E. Meyer, H.J. Güntherodt, A chemical sensor based on a microfabricated cantilever array with simultaneous resonance-frequency and bending readout, Sensors Actuators B: Chemical 77 (2001) 122–131.
[15] M.K. Ghatkesar, H.P. Lang, C. Gerber, M. Hegner, T. Braun, Comprehensive characterization of molecular interactions based on nanomechanics, PLoS ONE 3 (11) (2008) e3610, http://dx.doi.org/10.1371/journal.pone.0003610.
[16] H.P. Lang, M. Hegner, E. Meyer, C. Gerber, Nanomechanics from atomic resolution to molecular recognition based on atomic force microscopy technology, Nanotechnology 13 (2002) R29–R36.
[17] M.K. Ghatkesar, V. Barwich, T. Braun, J.P. Ramseyer, C. Gerber, M. Hegner, H.P. Lang, U. Drechsler, M. Despont, Higher modes of vibration increase mass sensitivity in nanomechanical microcantilevers, 445502 (8pp), Nanotechnology 18 (2007), http://dx.doi.org/10.1088/0957-4484/18/44/445502.
[18] S. Dohn, R. Sandberg, W. Svendsen, A. Boisen, Enhanced functionality of cantilever based mass sensors using higher modes, Applied Physics Letters 86 (2005) 233501–233503.
[19] D. Then, A. Vidic, C. Ziegler, A highly sensitive self-oscillating cantilever array for the quantitative and qualitative analysis of organic vapor mixtures, Sensors Actuators B: Chemical 117 (2006) 1–9.
[20] R. Mishra, W. Grange, M. Hegner, Rapid and reliable calibration of laser beam deflection system for microcantilever-based sensor setups, Journal of Sensors 2012 (2012) 617386.
[21] J. Mertens, M. Alvarez, J. Tamayo, Real-time profile of microcantilevers for sensing applications, Applied Physics Letters 87 (2005) 234102.
[22] P. Noy, R. Steiner, J. Voelkle, M. Hegner, C. Fattinger, Instrument for label-free detection of noncoding RNAs, Article ID 208079, 5 pages, Journal of Sensors 2012 (2012), http://dx.doi.org/10.1155/2012/208079.
[23] M. Dorrestijn, A. Bietsch, T. Acikalin, A. Raman, M. Hegner, E. Meyer, C. Gerber, Chladni figures revisited based on nanomechanics, Physical Review Letters 98 (2007) 026102, http://dx.doi.org/10.1103/PhysRevLett.98.026102.
[24] T. Braun, F. Huber, M.K. Ghatkesar, N. Backmann, H.P. Lang, C. Gerber, M. Hegner, Processing of kinetic microarray signals, Sensors and Actuators B: Chemical 128 (2007) 75–82.
[25] T. Braun, et al., Digital processing of multi-mode nano-mechanical cantilever data, Journal of Physics: Conference Series 61 (2007) 341.
[26] J. Jensen, M. Hegner, Predictions of the compressible fluid model and its comparison to experimental measurements of Q factors and flexural resonance frequencies for microcantilevers, Journal of Sensors 2012 (2012), http://dx.doi.org/10.1155/2012/258381, Article ID 258381, 7 pages.

Biographies

Jason Jensen studied theoretical and experimental physics and obtained his B.A. (mod) Hons. (Gold Medal) from the School of Physics in Trinity College Dublin in 2008. Since then he has been working as a Ph.D. student under the supervision of Prof. Martin Hegner in the Nanobiotechnology Group in CRANN.

Niall Maloney obtained his B.A. (mod) Hons. in Physics and Astrophysics from the School of Physics in Trinity College Dublin in 2008. Since then he has been working as a Ph.D. student under the supervision of Prof. Martin Hegner in the Nanobiotechnology Group in CRANN.

Martin Hegner received his M.Sc. in Life Science 1989, Swiss Federal Institute of Technology and his Ph.D. in Life Science 1994, Swiss Federal Institute of Technology. In 2006 he was awarded Endress professor for sensors in biotechnology at the University of Basel, Switzerland and in 2007 the professor at the school of Physics and CRANN institute of the Trinity College, Dublin, Ireland. His primary interests are related to the field of Nanobiotechnology, investigating single molecular interactions by optical tweezers and the development of nanomechanical diagnostic devices.